Hybrid System of Longitudinal CFRP Laminates and GFRP Wraps for Strengthening of Existing Circular Concrete Columns

Koosha Khorramian[1] and Pedram Sadeghian[2]

ABSTRACT: This paper presents an investigation on the behavior of a strengthening system of longitudinal premanufactured carbon fiber-reinforced polymer (CFRP) laminates and transverse glass FRP (GFRP) wrapping for strengthening of concrete columns (here after is called a hybrid system). The idea behind using the longitudinal CFRP strips was to enhance the system by increasing the flexural stiffness of the column which is effective for the strengthening of slender columns and eccentrically loaded columns where additional flexural stiffness is required for buckling control. The study was conducted experimentally in two phases under monotonic loads. Phase I was conducted on small-scale concrete specimens to characterize the hybrid system and phase II was conducted to verify the effectiveness of the hybrid system for the strengthening of large-scale slender concrete columns. In phase I, it was observed that by applying GFRP wraps on longitudinal CFRPs, the failure mode of CFRP laminates changed from buckling/debonding to crushing to achieve the full capacity of the system. However, as expected, test results in phase I showed that the usage of wrapping without longitudinal CFRP laminates was more effective than the proposed hybrid system for the strengthening of small scale concrete columns subjected to pure axial loading. For slender columns in phase II, the hybrid system enhanced the wrapping system by adding 52%, 105%, and 94% gain for axial capacity, flexural capacity, and lateral

---

[1] PhD Candidate, Department of Civil and Resource Engineering, Dalhousie University, D301, 1360 Barrington street, Halifax, NS, B3H 4R2 Canada, Koosha.Khorramian@dal.ca (corresponding author)

[2] Associate Professor and Canada Research Chair in Sustainable Infrastructure, Department of Civil and Resource Engineering, Dalhousie University, D403, 1360 Barrington Street, Halifax, NS, B3H 4R2 Canada, Pedram.Sadeghian@dal.ca

displacement at peak load, respectively, by altering the load-deflection curve of the slender columns to achieve a higher performance level.

KEYWORDS: CFRP laminate; GFRP wrap; hybrid; strengthening; concrete columns; slender; experimental; eccentric; concentric.

1. INTRODUCTION

During the past decades, fiber-reinforced polymer (FRP) composites have become widespread for the rehabilitation of existing concrete structures. One of the major applications of FRPs for construction has been known as the wrapping of concrete columns with FRPs to provide confinement for the concrete core. Wrapping of concrete columns enhances their axial load capacity and ductility [1, 2, 3, 4, 5, 6]. Therefore, FRP wrapping has been known very effective, especially for concentrically loaded columns [7, 8, 9, 10, 11]. However, for eccentrically loaded columns and slender columns, wrapping is not as effective as concentrically loaded columns. Parvin and Wang [12] recognized that wrapping of short concrete columns under eccentric compressive loading can successfully increase their capacity. However, Hadi [3] found out that the FRP wraps are effective for eccentrically loaded columns up to a certain margin. Bisby and Ranger [5] reported a reduction in the effectiveness of FRP wrapping for circular concrete columns loaded under combined axial and flexural loading. Al-Nimry and Soman [13] studied the slenderness effect of eccentrically-loaded circular concrete columns confined with FRP wraps and observed that the efficiency of the wraps in confining concrete columns decreases as the slenderness ratio increases. Also, ACI-440.2R-17 [14] limits the effective rupture strain of FRP wraps to 0.004 mm/mm where the load eccentricities are more than 10% of the diameter of the column. Moreover, ACI-440.2R-17 [14] is silent regarding slender columns. Since design of wrapping system tends to improve the columns providing confinement, the fiber orientation is set

to give the strong modulus of elasticity in the hoop direction. Thus, in many cases wrapping is used just unidirectionally in the transverse direction. Therefore, to increase the flexural stiffness, additional longitudinal reinforcement would be required for strengthening of eccentrically loaded columns or slender columns to overcome the limitation of the wrapping system.

In this paper, the system of longitudinal CFRP laminates and transverse GFRP wraps is called the hybrid system as two different components acts together and cause a unique behavior. The idea of a hybrid system, using high modulus longitudinal laminates such as CFRP premanufactured laminates, was to address the mentioned issue about wrapping and provide the required additional flexural stiffness to strengthen slender concrete columns where wrapping is not as effective, due to the nature of loading and secondary moment effects. Many researchers have evaluated the performance of CFRP laminates for concrete beams [15, 16, 17, 18, 19, 20, 21], concrete slabs [22, 23], and bridge decks [24, 25, 26]. However, the application of longitudinal CFRP laminates in compression for the strengthening of columns is limited by ACI 440.2R-17 [14] and CSA S806-12 [27] due to lack of experimental test data and its unknown behavior in structural applications for strengthening. On the other hand, recent studies on concrete columns strengthened with longitudinal FRPs [28, 29, 30, 31, 32, 33, 34, 35, 36, 37] as well as the columns which were built with FRP bars [38, 39, 40, 41, 42, 43, 44, 45, 46, 47] have shown the effectiveness of longitudinal FRPs in compression. Researchers found out that longitudinal layers of FRP improve the stiffness and moment capacity of the strengthened columns [48, 49, 4, 50, 29].

Application of near-surface mounted (NSM) CFRP strips for strengthening of columns was studied for short [34] and slender [28] columns showed an improvement of the column capacity. However, the limitation of spacing between the groove imposed by ACI 440.2R-17 [14] affects the number of strips that can be installed on the surface of concrete and limit the reinforcement ratio. The other solution is using FRPs bonded to the surface of the column to provide higher

reinforcement ratio. However, in compressive members, buckling and debonding of the bonded FRP laminates is expected which limits the effectiveness of the strengthening system. Therefore, providing lateral support for longitudinal FRPs should be considered as a solution that can be provided by wrapping. However, studies showed that providing lateral support was not enough to control the debonding or buckling of FRP laminates.

Khorramian and Sadeghian tested short rectangular [32] and circular [30] concrete columns strengthened with longitudinal bonded CFRP laminates and laterally supported with wraps or straps. The results showed an improvement in the column capacity. However, the occurrence of debonding of longitudinal CFRP laminates led to a sudden drop of the load. Thus, buckling was not controlled, and the premature debonding of FRP strips governed the system capacity before component level capacities were reached (i.e. crushing of longitudinal CFRP laminates, rupture of straps, rupture wrapping in hoop direction, or concrete crushing). Thus, there is room to improve the system to control the premature failure and reach the component level capacity which leads to higher reliability of the system and optimizing the material used for strengthening. In the previous research, the basalt FRP (BFRP) straps or partial wraps were used as the lateral support for the longitudinal CFRP laminates [32]. It was observed that even the existence of small gaps in the wrapping system (i.e. 46 mm) caused the debonding of CFPR laminates. Therefore, for the current study, the columns were fully wrapped, and the focus of the study was on preventing debonding of longitudinal CFRP laminates by examining a different number of layers for wrapping. The effect of confinement was separated from the effect of longitudinal laminates by performing separate tests on columns that were only wrapped.

Khorramian and Sadeghian [33] developed an analytical-numerical model and showed that eccentrically loaded slender concrete columns strengthened with the hybrid system of longitudinal CFRP laminates and transverse GFRP wrapping can be more effective than using conventional

wrapping system if premature failure is prevented. Therefore, the objective of this research is to validate the effectiveness of the hybrid system of longitudinal CFRP laminates and transverse GFRP wraps for slender concrete columns. Thus, two phases of experimental studies were designed. The validation of the system, mechanism of the hybrid system, and the requirements for reaching component level efficiency (i.e. finding the situation in which longitudinal CFRPs does not buckle) was investigated in phase I. Eighteen concrete columns strengthened with different combinations of longitudinal laminates and transverse wrapping were tested in phase I. Then, phase II of experimental tests, including three large-scale slender reinforced concrete columns strengthened with wrapping and hybrid systems, was designed and conducted to evaluate the effectiveness of the hybrid system for slender columns. It should be mentioned that phase I and II are completely different tests, since in phase I, the spceimens are unreinforced small scale concrete cylinders loaded concentrically, while in phase II, the specimens are large scale slender steel-reinforced concrete columns tested under eccentric loading. However, the concept of the hybrid system was used for strengthening of the specimens in both phases.

2. EXPERIMENTAL PROGRAM (PHASE I)

2.1. Test Matrix

In this phase, a total of eighteen circular cylinders (150 mm × 300 mm) strengthened with longitudinal CFRP strips, transverse GFRP wrapping, or a combination of both were prepared and tested under pure compression, as presented in Table 1. The specimens were divided into six groups, each consists of three identical specimens. The difference between testing groups was the variation in longitudinal and transverse strengthening systems as shown in Fig. 1. The specimen IDs were presented in the format of "x-wy-z", where "x" represents specimen type (i.e. "P" for plain concrete, "L" for longitudinally reinforced only, "T" for transversely reinforced only, and "H" for hybrid or combined reinforcement), "y" shows the number of wrapping layers, "w"

showed wrapping and is a fixed letter as a contraction for wrapping, and "z" shows the specimen number within the group as presented in Table 1.

2.2. Specimen Fabrication

Fig. 2 presents the process of specimen fabrication for typical specimens. For each longitudinally reinforced specimen, sixteen CFRP laminates with a rectangular cross-section (25 mm × 1.2 mm) were cut in strips with a length of 295 mm. The length of the longitudinal strips was considered less than the full length of the concrete specimens because of the prevention of strips from damaging the capping at the end of the specimens. The strips were considered slightly shorter than the length of the concrete cylinders to provide more room for adjustment as well as avoiding direct contact of CFRP strips with the loading system. To install CFRP strips, a compatible adhesive was applied to the surface of concrete and strips were positioned in a symmetric fashion using predefined guidelines on the surface. Afterward, two strain gauges were installed on CFRP strips which were on the opposite sides of the specimen. The surface of strain gauges was coated with a proper coating material and covered with an aluminum tape to be protected against resin for hybrid specimens.

For all wrapped specimens, the width of the GFRP fabric was the same as the height of concrete cylinders to provide full wrapping. Both two- and four-layer wrappings were continued to give 100 mm overlap at the end. To avoid premature failure at the ends of the specimens, the ends were strengthened using four layers of GFRP straps with a width of 30 mm. Finally, the surface of GFRP wraps was prepared and four more strain gauges were installed on the surface of the GFRP wraps (two in hoop direction and two in the axial direction).

2.3. Material Properties

For CFRP and GFRP materials, five tensile coupon tests were performed per ASTM D3039M-14 [51]. Table 2 presents a summary of the material properties for different elements used to build

the specimens including ultimate tensile strength f_t, modulus of elasticity E, and ultimate tensile strain ε_t. The average ± standard deviation of ultimate tensile strength, the tensile modulus of elasticity, and rupture strain of the tested specimens were 3267±348 MPa, 177.8±0.8 GPa, and 0.0179±0.0002 mm/mm, respectively, for CFRP strips while the mentioned values were 391±5 MPa, 25.7±2.4 GPa, and 0.0152±0.0011 mm/mm, respectively, for GFRP coupons based on the nominal ply thickness of 0.54 mm.

Five compression coupon tests were also conducted on an older batch of the CFRP laminates per ASTM D6641M-16 [52] whose results were presented in an earlier study [34]. It should be noted that these two products were from the same manufacturer and model. The results showed that the average modulus of elasticity of CFRP laminates in compression was only fourteen percent lower than that in tension. Moreover, the compressive strength of CFRP laminates was about one-third of their tensile strength. Thus, the compressive strength of CFRP strips was considered as 1089 MPa which is one-third of the tensile strength, the compressive modulus of elasticity considered as 152.9 GPa which is fourteen percent lower than the tensile modulus, and the ultimate crushing strain of CFRPs in compression was considered as 0.0071 mm/mm which is derived by dividing the compressive strength by compressive modulus of elasticity. The material characteristics for bonding adhesive which was used to install CFRP strips on concrete, and the properties of resin in wrapping are presented in Table 2, that reported by the manufacturer.

2.4. Test Set-up and Instrumentation

Fig. 3 presents the schematic test set-up used for testing the hybrid system. The test set-up components are spherical platen (which cancels accidental eccentricities), steel rings, and thick steel plate. It should be noted that all the tests were done under monotonic loading using a 2MN hydraulic actuator via a displacement control approach with a loading rate of 0.5 mm/min. For specimens in the longitudinal group (specimens with just CFRP strips), there were only two strain

gauges installed axially at the center of two opposite CFRP strips. For all wrapped specimens, there were two strain gauges installed axially on two opposite sides on the GFRP wrap as well as two strain gauges in the hoop direction.

In addition to strain gauges, four linear potentiometers (LPs) were installed for all groups of specimens. There were two steel rings in Fig. 3, which were installed on the specimens to make vertical LPs measure the relative axial displacement. The center of steel rings was the same as the center of the specimen, and they were bolted to the specimens to make a gauge length of 150 mm as shown in Fig. 3. It should be noted that LPs were necessary for capturing lateral strain of specimen built with only with plain concrete or the ones with only longitudinal CFRP strips. However, the LPs were used during the testing as a controlling tool for strain gauges. A data acquisition system with a frequency of 10 Hz recorded the strain, load and displacement values.

3. EXPERIMENTAL RESULTS AND DISCUSSION (PHASE I)

A summary of the test results including the axial stresses, average of the hoop strains, and average of axial strains are presented in Table 3. For specimens with two layers of wrapping, the average peak load for the hybrid, longitudinal, and wrapped systems are 1274.7 kN, 1160.8 kN, and 1246.5 kN, respectively, which are corresponding to 26.9%, 15.6%, and 24.1% enhancement of capacity with respect to the plain concrete. For specimens with four layers of wrapping, the average peak load for the hybrid and wrapped systems were 1700.4 kN and 1761.4 kN, respectively, which are corresponding to 69.3% and 75.4% enhancement of capacity with respect to the plain concrete. It should be noted that the use of two and four layers of wrapping, caused 15.6% and 46.5% gain of strength with respect to the plain concrete, respectively. Therefore, it was observed that adding wrapping to longitudinal CFRP strips drastically increased the capacity of the columns. However, the wrapped system is more effective in increasing the capacity of the columns without longitudinal CFRP strips.

The average capacities, gain in the capacity, the average longitudinal strains, and the average lateral strains are presented in Table 4. The results showed that wrapped only group reached the peak load with 0.00540 mm/mm and 0.00959 mm/mm more longitudinal and lateral strains with respect to the hybrid system with two layers of wrapping, respectively, and 0.00646 mm/mm and 0.00766 for four layers of wrapping. Thus, the average strain recording at peak load showed that the hybrid system experienced much less longitudinal and lateral strains than the wrapped system at the peak load. Also, the results showed that the longitudinal only system and hybrid system with two layers of wrapping experienced less longitudinal strain than the plain group. However, the wrapping caused an increase in lateral and longitudinal strains of the hybrid system with respect to only longitudinal system once the number of wrapping layers increased. Therefore, the gain in the capacity and increase in lateral and longitudinal strain with increasing the number of wrapping layers improved the overall behavior of the hybrid system. This improvement changed the modes of failure, as well, which is discussed in the following section.

3.1. Failure Modes

Fig. 4 presents four different types of failure corresponding to different reinforcement systems. As shown in Fig. 4(a), the longitudinal specimens (i.e. specimens that were only reinforced with longitudinal strips) were experienced debonding of the CFRP strips from the concrete specimens at the peak load which followed by a sudden drop in load-bearing capacity and buckling of CFRP strips. The capacity and stiffness of the specimens in the longitudinal group were enhanced in comparison to the plain specimens, although they were limited due to lack of lateral support for longitudinal CFRP strips and debonding. By strengthening longitudinal CFRP strips with 2 layers of GFRP wrapping, their axial capacity improved. However, there were observations that showed CFRP strips did not reach their crushing capacity and instead debonding cause separation between CFRP strips and concrete. Fig. 4(c) shows the rupture of GFRP wrap for the hybrid system with

two layers of wrapping, which was localized over one of the CFRP strips. It was possible that the debonding of CFRP laminate caused the buckling of one of the strips and formed a longitudinal pattern of rupture in GFRP wrapping. On the other hand, the specimens which were reinforced with only wrapping in hoop direction (both two and four layers of wrapping) show rupture of GFRP wrapping at the middle height of the specimen, and propagation of cracks in GFRP wrapping was along the hoop direction as shown in Fig. 4(b). Therefore, the localized longitudinal rupture pattern of GFRP wrapping in hybrid specimens with two layers of GFRP wrapping can be attributed to the debonding of longitudinal CFRP strips and their buckling afterward. On the contrary, for hybrid specimens wrapped with four layers of GFRP, there was no observation of a longitudinal rupture pattern of GFRP wrapping. Instead, a rupture pattern similar to wrapped only specimens was observed as shown in Fig. 4(d). Moreover, more evidence confirmed that idea after observing the specimen after failure; crushing of longitudinal CFRP strips was observed inside the GFRP wrapping. Also, the capacity of these specimens was significantly improved in comparison to the longitudinal or hybrid specimens with two layers of GFRP wrapping. Thus, providing specimens with more lateral support (i.e. using four layers wrapping instead of two layers) alternated the mode of failure from CFRP debonding and buckling to CFRP crushing. It can be concluded that minimum lateral support by GFRP wraps was needed to ensure CFRP strips reach to crushing rather than their debonding and buckling (which cause a premature rupture for the GFRP wrap). Later in this paper, the mechanism of the failure is explained and verified.

3.2. Load-Strain Behavior

Fig. 5 presents the load-strain curves of all specimens. The average load-strain curves and the capacity of each group of specimens are presented in Fig. 6. Test results showed that the slope of load-strain curves for all specimens reinforced with longitudinal CFRP strips (i.e. L-w0, H-w2, and H-w4 groups) was higher than other specimens. In other words, it was observed that L-w0, H-

w2, and H-w4 groups experienced the same loading history up to failure, as shown in Fig. 6(a). As the strain in the specimens increased, due to the dilation of the concrete, the tendency for debonding of CFRP strips increased. Thus, the specimens which were not supported laterally (i.e. L-w0 group) experienced debonding of CFRP laminates following by their buckling before reaching the CFRP crushing strain. By adding 2 layers of GFRP wrapping, the lateral support for specimens in the H-w2 group was improved in comparison to the L-w0 group and they were able to sustain more load before failure and they failed at a higher strain level. Considering even two more layers of wrapping (i.e. four layers of GFRP wrapping) showed that even higher strain levels can be reached. The additional GFRP layers cause a decrease in concrete dilation and provide lateral support for the CFRP strips which, in turn, enable CFRP strips to sustain loads up to their crushing strain without experiencing any debonding or buckling. Therefore, the hybrid system was able to reach the maximum component level capacity (i.e. crushing of CFRP laminates).

The load-strain curves in Fig. 5 show that there is strain hardening behavior for only wrapped specimens (i.e. T-w2 and T-w4) as well as hybrid specimens wrapped with four layers of GFRP (i.e. H-4w). It should be noted that the presence of the GFRP wraps, in addition to providing lateral support for the CFRP strips, provides confinement for the hybrid specimens with four layers of GFRP wrapping. However, for the hybrid specimens with two layers of wrapping, the load-strain curves showed a drop after the peak load which was considered with debonding and buckling of CFRP strips. Thus, load-strain curves showed two different behavior for the hybrid system which depends on layers of GFRP wrapping.

The average gain in the capacity of each group of the tested specimens is presented in Fig. 6(b). The capacity of the hybrid specimens did not reach the capacity of the wrapped specimens with similar GFRP wrapping although the hybrid system with four layers of wrapping was successfully able to survive up to the crushing capacity of CFRP strips. The reason behind this

difference in capacity is the difference between the modes of failure. While, for the wrapped specimens, the rupture of GFRP wrapping was corresponding to the peak load, for the hybrid specimens either debonding or crushing of CFRP strips caused failure initiation at peak load at lower levels of strain. Therefore, for the hybrid system, the controlling part is longitudinal CFRP strips while GFRP wrapping are supporting longitudinal elements. The presence of GFRP wrapping is more important for the prevention of debonding and buckling of CFRP laminates. Thus, more layers of GFRP wrapping would not be economically proper for this system, since way before reaching the rupture of GFRP wrapping, CFRP laminate would be crushed. At the same time, fewer layers of GFRP wrapping would lead to debonding and buckling of CFRP laminates. Determination of this limit requires a solid experimental database that is out of the scope of the current study. However, this study showed that this limit exists, and that the system can be optimized to reach the component level capacity. From the results of phase I, it can be concluded that wrapping system is more appropriate than the hybrid system for strengthening of concentrically loaded concrete columns. However, for slender and eccentrically loaded columns, the hybrid system would be more effective by providing more flexural stiffness controlling the second order deformation of slender columns as presented in phase II.

3.3. Confinement Effect

To study the effect of confinement in the hybrid system, the confining pressure of the tested specimens wrapped with GFRP were calculated using three different values as effective strain: a) the ultimate tensile strain found from the tensile test of coupons ($\varepsilon_{fe} = \varepsilon_{frp}$); b) the suggested effective strain suggested by ACI 440.2R -17 [14] as 55 percent of the ultimate tensile strain ($\varepsilon_{fe} = 0.55\,\varepsilon_{frp}$); c) the hoop rupture strain of GFRP wraps at the time of failure or peak load ($\varepsilon_{fe} = \varepsilon_{h,rup}$). The confining pressure (f'_l) was calculated based on Eq. 1 per ACI 440.2R-17 [14].

$$f'_l = \frac{2E_f t_f \varepsilon_{fe}}{D} \qquad\qquad (1)$$

where D is the diameter of the concrete column (150 mm), E_f is the modulus of elasticity of GFRP wrap (25.7 GPa), t_f is the total thickness of GFRP wrapping (0.54 mm per layer), and ε_{fe} is the effective strain of GFRP wrapping. The calculated values for the confining pressure are presented in Table 5. Per ACI 440.2R-17 [14], there is a limit of 0.08 for confining pressure (f'_l) over the unconfined concrete strength (f'_{co}) after which the confinement is considered as effective. If the confinement ratio (f'_l/f'_{co}) is greater than 0.08, the stress-strain curve of confined concrete with FRP wrapping may have a descending branch. For two layers of wrapping, wrapped only specimens reached higher confinement limit than 0.08 in the tests and their stress-strain curves did not experience a descending branch and reached higher capacity than unconfined concrete strength while for the hybrid system the confinement ratio calculated from hoop rupture strain dd not pass the limit of 0.08. Therefore, the confinement was considered enough to be effective for wrapped specimens, but not for the hybrid specimen with two layers of wrapping. Once four layers of wrapping used, both groups showed confinement ratios higher than 0.08 as expected. Therefore, in this study, the confinement was considered as "activated" for four layers of wrapping and as "not activated" for two layers of wrapping for the hybrid system.

Also, the confined concrete strength (f'_{cc}) is presented in Table 5. For only wrapped specimens, the confined concrete strength was calculated simply by dividing the axial capacity recorded at the peak load by the cross-sectional area of the columns. However, for hybrid specimens, the effect of CFRP strips was deducted from the peak load to separate the confining effect and the effect of the longitudinal CFRP strips. The material tests showed that the stress-strain curve for FRPs is linear. Thus, the contribution of the CFRP strips (P_{CFRP}) was calculated by multiplying the cross-sectional area of all CFRP strips (A_{CFRP}), the modulus of elasticity of

CFRP strips (E_{CFRP}), and the average value of strain recorded at the peak load (ε_{CFRP}), presented in Eq.2. The contribution of CFRP strips was deducted from the peak load (P_u) to give the load corresponding to the confined concrete ultimate load (P_{cc}), which in turn gives the confined concrete strength (f'_{cc}) by being divided by the cross-sectional area of the concrete column (A_c), presented in Eq.3 and Eq.4.

$$P_{CFRP} = A_{CFRP} \times E_{CFRP} \times \varepsilon_{CFRP} \tag{2}$$

$$P_{cc} = P_u - P_{CFRP} \tag{3}$$

$$f'_{cc} = \frac{P_{cc}}{A_c} \tag{4}$$

The results showed that the average confined concrete strength for only wrapped specimens and hybrid specimens were 70.5 MPa and 60.9 MPa for two layers of wrapping, respectively, and 99.7 MPa and 65.6 MPa for four layers of wrapping. By deducting the concrete strength for unconfined concrete (56.8 MPa), the gain in strength due to the presence of confining pressure for wrapped only specimens was determined as 13.7 MPa and 42.9 MPa, for two and four layers of wrapping, respectively. It should be highlighted that for the hybrid system, these values are only 4.1 MPa and 8.8 MPa for two and four layers of wrapping, respectively. In other words, it was observed that the additional gain in strength due to wrapping for the hybrid system was reduced to 29.6% and 20.4% of the only wrapped system for two and four layers of wrapping, respectively. On the other hand, although the gain due to GFRP wrapping is reduced as wrapping layers increases, the wrapping served as the lateral support for the CFRP strips and assisted CFRP strips to sustain higher strains before peak load and to reach their ultimate compressive capacity by changing the mode of failure from debonding/ buckling of strips to crushing of them. Since the capacity of the hybrid system was more than only wrapped system for two layers of wrapping and was almost comparable to that for four layers of wrapping, the longitudinal CFRPs were effective

and considerably contributed to the strength gain for the hybrid system. The latter is studied more in the following section by showing the mechanism of the hybrid system.

4. FAILURE MECHANISM (PHASE I)

In this section, an analytical approach is presented to determine the mechanism of the hybrid system through a cross-section analysis isolating the contribution of longitudinal CFRP strips and concrete core confined with transverse GFRP wraps. Fig. 7 shows the typical load-strain curves of longitudinal CFRP strips, unconfined concrete, and confined concrete. To derive the load-strain curves, the loads at each strain can be derived by considering that a perfect bond is between CFRP laminate and concrete. Thus, at a certain axial strain, the stress of each component (i.e. concrete or CFRP laminates) can be found from the stress-stress curve of each component, and then by multiplying the area of each component by their corresponding stress the corresponding loads can be calculated. The stress-strain relationship of the CFRP laminates was considered linear elastic. For unconfined concrete, the stress-strain curve proposed by Popovics [53] was adopted while for confined concrete, the model proposed by ACI 440.2R [14] was used.

Two different scenarios can be introduced regarding the contribution of GFRP wrapping in the hybrid system depends on whether the wrap is activated or not activated, as shown in Fig. 7. As it was observed in Fig. 6(a), for the specimens with four layers of GFRP wrapping, there is a secondary slope in the load-strain curves which shows the confinement effect was contributed to the capacity (this case is named as an activated wrap in this study). However, for two layers of wrapping, there was no observation of the secondary slope in load-strain curves and no confinement effect was observed (this case is named as a not activated wrap in this study). The slope of load-strain curves was higher for all specimens with longitudinal CFRP strips while for the wrapped specimens the slope was the same as plain concrete specimens. The latter implies that in all hybrid specimens, CFRP was contributing to the load-carrying capacity. However, the

system experienced failure once CFRP strips were deboned/ buckled or crushed. It was observed that for the specimens with two layers of GFRP wrapping, the concrete was controlling the failure instead of CFRP strips. At the strain corresponding to the peak load of unconfined concrete, the debonding of CFRPs happened. For deriving the load-strain curve, if the load of unconfined concrete and CFRP strip were added at each strain level to give the total load of the hybrid system (without wrap activation), the debonding would happen at a strain corresponding to the peak load of unconfined concrete, as shown in Fig. 7. In this case, the unconfined concrete wants to expand as the strain increases and after peak load the rate of expansion increases which causes the elimination of the bond between CFRP and concrete as well as the failure of the system. Moreover, the lateral support provided by two layers of wrapping is not sufficient to prevent the expansion of concrete. However, this lateral support causes a delay in the debonding of CFRP strips for two layers of GFRP wrapping in comparison to specimens without any lateral support. Fig. 6(a) shows that the concrete specimens wrapped with longitudinal CFRPs with or without wrapping followed the same path in the load-strain curves, but the ones without any lateral support experience debonding of CFRPs earlier. In contrast, when there is enough lateral support, CFRPs continue to sustain loads after the peak load of unconfined concrete and even showed a secondary branch in their load-strain curves. The latter shows that both wrapping and CFRP laminates were effective in the load-carrying capacity of the system for this case. Therefore, to derive the load-strain curve of this case CFRP laminate load can be added to the confined concrete load to give the total load for the hybrid system (with wrap activation). The failure of the system governs by crushing of longitudinal CFRP laminates.

The verification of the explained mechanism is presented in Fig. 8, where the experimental load-strain test results and the prediction of the results based on the hybrid mechanism are in a very good agreement. As shown in Fig. 8(a), for four layers of GFRP wrapping, the load at each

strain can be calculated by combining the confined concrete and longitudinal CFRP strip loads up to crushing. In this case, the GFRP wrapping not only provides enough support for longitudinal CFRP to last up to its crushing but also provides confinement effect. Therefore, the dilation of concrete can be controlled by the confinement effect which prevents the debonding of CFRPs in turn. However, as shown in Fig. 8(b), two layers of GFRP wraps were not able to provide enough lateral support for the concrete core and longitudinal CFRP strips, and the debonding of the strips at the peak load controlled the capacity of the specimens according to both experimental and analytical results.

Overall, the hybrid system is validated for concrete columns loaded axially, and it was observed that enough layers of wrapping (which is correlated to the amount of confining pressure provided by confining device) make it possible for CFRP strips to reach the crushing strength in compression without buckling. Also, the system gains from both wrapping and longitudinal strips, but up to the crushing of the CFRP strips. Therefore, for pure compression, only wrapped system is more effective since there would be no interruption for GFRP wraps to reach higher strains and to give higher capacities. However, for slender columns or eccentrically loaded columns, where wrapping was not recognized as effective as in pure compressive loading, the hybrid system is expected to increase the capacity of the system due to providing additional flexural stiffness for the concrete column while longitudinal strips can reach their capacities due to presence of wrapping. Therefore, in the following section, the hybrid system application for slender columns is validated through experimental tests and is compared to the wrapped only system.

5. LARGE-SCALE VALIDATION OF HYBRID SYSTEM (PHASE II)

5.1. Description of Phase II Tests

Three slender circular reinforced concrete columns (260 mm diameter) with the length of 3048 mm were built and tested in phase II of the studies. The design considerations were considered per

ACI 318-19 [54]. Six 15M steel rebar were used as longitudinal reinforcement and twenty 10M ties were considered as ties. The spacing of ties was 203 mm at the middle of the column and reduced to 102 mm at the distance of 610 mm at the end of the columns. The specimens were cast with normal concrete with a strength of 30 MPa which is close to the concrete strength of aged structures. The rest of the material characteristics are the same as explained in Table 2.

5.1.1 Test Matrix and Fabrication

The test matrix is presented in Table 6. Three specimens were considered: 1) Control specimen was considered without strengthening; 2) Wrapped specimen was considered with six layers of GFRP wrapping with 100 mm overlap; 3) Hybrid specimen was considered with sixteen longitudinal CFRP strips (50x1.2 mm) and six layers of GFRP wrapping. While 6 layers of GFRP wrapping (f'_l = 5.35 MPa) was used for the large-scale specimens in phase II, 4 layers of wrapping (f'_l = 6.19 MPa) was used for small scale specimens in phase I. However, for the phase II, specimens were not intended to be replicated from phase I, and the purpose was only the evaluation the system for small scale and large scale specimens. It should be mentioned that the reinforcement ratio of longitudinal CFRPs was reduced from 2.7% for phase I to 1.8% for phase II. Also, the gap between the longitudinal CFRP strips was 18% in phase I and 2% in phase II. All the gaps were carefully filled with the adhesive to avoid sharp corners and make a smooth surface before the application of the wraps. It should be highlighted that the two phases of this study were not supposed to be similar. In phase I the compression behavior of the longitudinal laminates was the target of evaluation to design the large scale tests of phase II.

The preparation of the specimens is similar to the explained process for phase I. Fig. 9 showed the preparation stages of the hybrid specimen. GFRP wrapping was installed in two stages due to the length of the column, as presented in Fig. 9(c). For all three specimens, an additional three layers of wrapping were considered for the ends of the specimens to avoid premature failure

of the column ends as presented in Fig. 9(d). Also, the end wrapping with three layers of GFRP with a length of 305 mm   at the top of 6   layers of continuous GFRP wraps, provided enough anchorage for the longitudinal strips as there was no anchorage failure during the tests. More research is needed to determine the minimum required end wraps for different cross-sections, reinforcement ratios, and slenderness ratios.

5.1.2 Test Set-up and Instrumentation

Fig. 10 presents the test set-up and instrumentation for phase II. The specimens were tested horizontally due to limitations in the lab. However, the test set-up was used by the authors' research group and its accuracy for this test was approved [55, 56]. The test set-up consists of two strong concrete cubes named "End blocks" which were tightened to the strong floor. Between these two end blocks, the load is applied to the system via a 2MN Instron actuator whose force is recorded by the load cell, as shown in Fig. 10. The columns were loaded using a displacement control approach with a rate of 2 mm/min. The load transfers from the actuator to a shaft, whose direction of movement is controlled by a tunnel, and applied axial load to the concrete column. To provide load eccentricity, two rollers were considered at the ends of the specimen whose distance from the center of the columns gives the desired eccentricity. The rollers are in contact with a v-notched plate which allows the specimen to rotate to provide simply supported boundary conditions. To provide a specimen with easier movement and to cancel the effect of the wight of the column in the horizontal direction, two sets of steel balls were provided for the specimen that allows lateral movement, as shown in Fig. 10. To record the data, two string pods (SPs) and two linear potentiometers (LPs) were installed at the mid-section of the column to record the lateral displacement. Also, a total of ten strain gauges were installed to record the axial strain in compression and tension sides on steel bars, CFRP strips, and GFRP wrapping, and to record the strain of GFRP wrapping in the hoop direction.

5.2. Results and Discussion

A summary of the test results for phase II of the experimental tests is presented in Table 7. The results showed a considerable gain in the axial and bending moment capacity of the hybrid strengthening system in comparison to the wrapping system. The strain values showed that steel rebar in compression was yielded for all specimens, while tensile strain values of steel rebar at the peak load show that the hybrid system reached higher tensile strains than the wrapping system. Also, the confining strain was higher for the hybrid system at the peak load in comparison to the wrapping system. In the following the modes of failure, loading path, and load displacement of the specimens are discussed, and the effect of the hybrid system and wrapping system is compared.

5.2.1 Failure modes

Fig. 11 shows the failed specimens and the modes of failure. For the control specimen, the loading continued up to the column reached concrete crushing at the middle of the column, as presented in Fig. 11(a) and 11(d). After concrete crushed, there was a sudden drop in the axial load as for the control specimen and there was no descending branch in its load-displacement curve, as presented in Fig. 12(a). The wrapped specimen did not reach the material failure at its peak load and failed due to the global buckling of the column as presented in Fig. 11(b). After buckling, loading continued and the specimen tolerated loads which led to a smooth and long descending branch of the load-displacement curve, and the test finally stopped by the operator due to considerable lateral displacement. It should be mentioned that GFRP wrapping did not rupture. Instead, the matrix failure happened which showed matrix crushing in the compression side, as presented in Fig. 11(b), and matrix rupture in tension side, as presented in Fig. 11(e). The hybrid specimen started its load-displacement curve with a higher slope due to the presence of longitudinal CFRP strips, as presented in Fig. 12(a). The hybrid system reached its peak load once the CFRP strips at the compressive side crushed which was accompanied by a noise, as presented in Fig. 11(g). It should

be highlighted that no sign of buckling or debonding of CFRP strips was observed up to the peak load. After peak load, the CFRP at the middle of the column in the compression side was debonded and initiated some small cracks in the GFRP wrapping which was progressed up to reaching the rupture of GFRP wrap, as presented in Fig. 11(f). Once GFRP ruptured the axial load dropped with a steep slope which leads to total failure of the column, as presented in Fig. 12(a) and Fig. 11(c).

5.2.2 Comparison of Hybrid and Wrapping Systems

The loading path (i.e. axial load-bending moment curve) and interaction diagram for the tested specimens are presented in Fig.12 (b). To find the bending moment (M) for each specimen, the load (P) was multiplied by the sum of initial eccentricity (e_0) and the lateral displacement (Δ) at the middle of the columns (i.e. $M = P(e_0 + \Delta)$). The detailed procedure for deriving the interaction diagram for the hybrid system is explained by Khorramian and Sadeghian [33]. However, the confinement model used in the mentioned study was adopted from ACI 440.2R-17 [14] which has limitations and was constant for by changing the eccentricity and did not allow to consider the confinement effect for eccentricity for diameter ratios of higher than 10 percent. However, in this study, the confinement model was updated to consider the effect of eccentricity in the confined stress-strain curve using the variable confinement model proposed by Lin and Teng [57]. Due to the mechanism of the hybrid system observed in phase I and confirmed in phase II, the hybrid system is not able to reach higher strength after the crushing of CFRP laminates occurs. Therefore, there is a cut-off part for the interaction diagram of the hybrid system which is corresponding to reaching CFRP crushing in the compression side. It was also observed from the calculation of the interaction diagram that higher for higher eccentricities there is a possibility in changing the failure mode of the hybrid system from crushing of CFRP laminates in compression to their rupture in tension, as presented in Fig. 12(b). It was observed that the hybrid system improved the interaction diagram and loading path of the strengthening system drastically in comparison to the wrapping

system. Also, the interaction diagrams showed that the hybrid system is more effective as the bending moment increases and less effective as the column tend to be concentrically loaded since for concentric loading CFRP strips in compression would reach their crushing early (see the cut-off of interaction diagram) and the gain in strength would be negligible in comparison to the wrapping system, as experienced in phase I of the study. Therefore, as eccentricity increases, the effectiveness of the system increases.

To find points for the interaction diagram, material properties presented in Table 2 were considered in the calculation. For the interaction diagram of the wrapping system, the strain at the furthest compressive fiber of concrete was set to the axial strain corresponding to the rupture of GFRP wrap for each eccentricity. The intersection of the experimental loading path and the interaction diagram was determined as the predicted rupture point of the GFRP wrap as shown in both loading path and load-displacement curves with a white circle in Fig. 12. As explained earlier, the wrapping system failed due to global buckling, which is reflected in its loading path as it reaches the peak load before touching the interaction diagram and reach the interaction diagram in its descending branch. After reaching the interaction diagram (predicted GFRP rupture), the wrapped specimen showed a backward trend in the loading path which means the moment capacity is lost due to experiencing excessive lateral displacements.

For the hybrid system, three different interaction diagrams were calculated, as shown in Fig.12(b), which consider: a) only crushing of CFRP strips in compression (blue line); b) only rupture of GFRP wrap in tension without crushing of CFRP (red line); c) rupture of GFRP wrapping after two furthest layers of CFRP strips were crushed in compression (black line). The predicted CFRP crushing point (gray circle in Fig. 12) was determined as the intersection of the experimental loading path of the hybrid system and the interaction diagram which considered only the crushing of two furthest layers of CFRP strips. The test results showed that the observed peak

load is higher than the predicted one, which means the CFRP laminates in compression were able to reach and pass the material level crushing strain. The latter is due to the presence of sufficient confinement for the CFRP wraps which was not available in the material testing. Therefore, the result of the phase I test is validated for the slender column tested in phase II although the confining pressure is even less. Also, the results showed that the hybrid system would not lose the full axial and flexural capacity after some of the CFRP strips crushed, and the system continues to resist up to the rupture of GFRP wrap. It should be highlighted that for the hybrid system, the predicted rupture of GFRP wrap and the actual rupture of GFRP wrapping occurred at the same time. This validates the mechanism of the hybrid system for the slender column and shows that the interaction diagram corresponding to the crushing of CFRP laminate and then rupture of GFRP wrap (the black interaction diagram) represents the mechanism of the test. Similar to the wrapping system, after specimen reached the rupture of GFRP wrapping the loading path moved backward for the hybrid system and the flexural capacity dropped drastically due to a sudden drop in the axial load.

Fig. 13 presents the gain in the capacity of the hybrid and wrapped strengthening specimens from the control specimen. The results showed that the gain in the axial capacity, in flexural capacity, and in sustaining lateral displacement were 70%, 136%, and 130% for hybrid specimen, respectively, while they were 18%, 31%, and 37% for the wrapped specimen. The extra gain in the capacity of the hybrid system is attributed to the presence of the longitudinal CFRP strips. Thus, the results showed that the hybrid system enhanced the wrapping system by 52%, 105%, and 94% for axial capacity, flexural capacity, and lateral displacement, respectively. Therefore, the hybrid system improved the system performance considerably.

6. FUTURE RESEARCH

In this study, only two different levels of confinement (i.e. 2 and 4 layers of GFRP wrapping) were considered for phase I. However, a confinement limit is required to determine if the hybrid

mechanism should be considered with or without an activated wrapping effect. Moreover, this limit would be very economically effective since extra layers of wrapping would not lead to considerable change in the capacity of the system because the system is controlled by CFRP crushing if lateral support is enough. It should be also noted that for wrapped concrete columns, there is a limit of 0.08 for confinement pressure over unconfined concrete strength that was defined by ACI 440.2R [14]. The formula was derived based on experimental observations as well as using a mathematically derived formula for the collected database for confined concrete columns. Their major criterion was to find the confinement levels that make the corresponding strength to the FRP hoop rupture strain equal to or greater than the unconfined concrete strength [58, 59]. However, the presence of CFRP strips between concrete and GFRP wrapping in the hybrid system, make the situation more complicated since there might be no corresponding point to the rupture of GFRP wrapping since longitudinal CFRP failure, due to crushing or debonding, is before wrapping failure. Therefore, to establish the limit that dictates wrap activation, further studies and experimental evidence are required, and more experimental data assist in building a database and find the limit. It should be highlighted again that the experimental program was intended to characterize only the behavior of the hybrid system in the component level and check the validity of its performance for small scale columns and extend it to slender columns. However, the main application of the hybrid system is to enhance the performance of slender columns and to improve eccentrically loaded columns that require flexural stiffness. The latter requires further experimental studies and verification. Therefore, more large scale slender columns are required to be tested with various eccentricities, slenderness ratios, reinforcement ratios, and wrapping layers to give more comprehensive conclusions. Also, a numerical-analytical study would help to perform further analysis and doing a parametric study. A comprehensive second order analysis is required to complete the investigation to create a data platform on the behavior of the hybrid

strengthening system assisting the development of design recommendations and simplified methods. However, the number of tests on the subject is limited and more experimental is required to characterize the behavior of the hybrid system. Therefore, more large-scale experimental tests on the behavior of slender concrete columns strengthened with the proposed hybrid system is crucial to continue the current study. Furthermore, a reliability analysis will be required to assess the safety of the proposed hybrid system for design applications. Also, it is recommended to further validate the performance of the system for earthquake resistant structures by conducting cyclic loading and considering variable reversal eccentricities. All the mentioned areas of research are out of the scope of the current study and should be addressed in future studies.

7. CONCLUSION

In this study, a total of eighteen small scale concrete columns were tested under pure axial loading up to failure in phase I, and a total of three slender full-scale concrete columns were tested under eccentric loading in phase II to evaluate the effectiveness and performance of a hybrid strengthening system of longitudinal bonded CFRP laminates laterally supported with GFRP wrapping. It should be mentioned that in the two phases of this study, different specimens with different reinforcement, slenderness ratio, and load eccentricity were considered, but the same concept of hybrid strengthening system was used for both phases. Phase I was designed to characterize the behavior of the hybrid system at small scale level ensuring the longitudinal laminates have enough lateral support from the wraps preventing the local buckling of the laminates. Also, the crushing behavior of the laminated were evaluated under the condition of the lateral support from the wraps. Then the system was used in phase II to evaluate the behavior of the system on large scale columns controlling the global buckling of slender columns. The following conclusions can be drawn:

- The hybrid system was not efficient in small scale axially loaded concrete columns since the capacity is controlled by the crushing of CFRP laminates and did not allow the system to reach the full capacity of the GFRP wrapping.

- For axially loaded small scale concrete columns, two major modes of failure for the hybrid system were observed: i) debonding of CFRP laminates following by rupture of GFRP wraps, and ii) crushing of CFRP laminates followed by rupture of GFRP wraps. The mode of failure changed as the number of GFRP wrapping increased and caused the mode of failure change from buckling/debonding of CFRP strips to crushing of CFRPs in compression followed by the rupture of GFRP wrapping.

- For eccentrically loaded slender columns, the hybrid system was considerably more effective than the wrapping system due to increasing flexural stiffness and controlling of second-order deformations. The hybrid system enhanced the wrapping system by adding 52%, 105%, and 94% gain for axial capacity, flexural capacity, and lateral displacement at peak load, respectively.

- The failure of the hybrid system for slender columns occurred in two stages: i) the CFRP laminate in compression reached its ultimate crushing capacity at the peak load; ii) the column continues to sustain loads up the final failure caused by the rupture of GFRP wrapping at the middle of the column.

- It should be noted that the conclusion of this study is valid in the range of the tested specimens in phase I and phase II of the experimental studies. For more in-depth understanding of the strengthening system, future studies using different materials, dimensions, loading protocols are required.

- This study was the experimental validation of the performance of the hybrid system and more evidence is required for more in-depth understanding of the system. Thus, further

studies are required to assess the activation limit of the hybrid system and its application for the strengthening of slender concrete columns by conducting more experimental tests. A comprehensive second order analysis on the behavior of the strengthening system should be developed to perform a parametric study and suggestion for design applications. Also, safety and reliability based analysis is required to assess the safety of the studied hybrid system.

8. ACKNOWLEDGMENT

9. REFERENCES

[1] A. Nanni and N. Bradford, "FRP Jacketed Concrete under Uniaxial Compression," *Construction and Building Materials,* vol. 9, no. 2, pp. 115-124, 1995.

[2] H. A. Toutanji, "Stress-Strain Characteristics of Concrete Columns Externally Confined with Advanced Fiber Composite Sheets," *ACI materials journal,* pp. 397-404, 1999.

[3] M. N. S. Hadi, "Behaviour of FRP Wrapped Normal Strength Concrete Columns under Eccentric Loading," *Composite Structures,* vol. 72, no. 4, pp. 503-511, 2006.

[4] P. Sadeghian, A. R. Rahai and M. R. Ehsani, "Experimental Study of Rectangular RC Columns Strengthened with CFRP Composites Under Eccentric Loading," *Journal of Composites for Construction,* pp. 443-450, 2010.

[5] L. Bisby and M. Ranger, "Axial–flexural Interaction in circular FRP-Confined Reinforced Concrete Columns," *Construction and Building Materials,* vol. 24, no. 9, pp. 1672-1681, 2010.

[6] F. Yu, G. Xu, D. Niu, A. Cheng, P. Wua and Z. Kong, "Experimental Study on PVC-CFRP Confined Concrete Columns under Low Cyclic Loading," *Construction and Building Materials,* vol. 177, p. 287–302, 2018.

[7] S. Pessiki, K. A. Harries, J. T. Kestner, R. Sause, and J. M. Ricles, "Axial Behavior of Reinforced Concrete Columns Confined with FRP Jackets," *Journal of Composites for Construction,* vol. 5, no. 4, pp. 237-245, 2001.

[8] . T. Ozbakkaloglu, "Compressive Behavior of concrete-filled FRP Tube Columns: Assessment of Critical Column Parameters," *Engineering Structures,* vol. 51, pp. 188-199, 2013.

[9] Y. Xiao and H. Wu, "Compressive Behavior of Concrete Confined by Carbon Fiber Composite Jackets," *Journal of materials in civil engineering,* vol. 12, no. 2, pp. 139-146, 2000.

[10] C. Cui and S. A. Sheikh, "Cui, C., and S. A. Sheikh. "Experimental study of Normal-And High-Strength Concrete Confined with Fiber-Reinforced Polymers," *Journal of Composites for Construction,* vol. 14, no. 5, pp. 553-561, 2010.

[11] S. T. Smith, S. J. Kim, and H. Zhang, "Behavior and Effectiveness of FRP Wrap in the Confinement of Large Concrete Cylinders," *Journal of Composites for Construction,* vol. 14, no. 5, pp. 573-582, 2010.

[12] A. Parvin and W. Wang, "Behaviour of FRP jacketed concrete columns under Eccentric Loading," *Journal of Composites for Construction,* vol. 5, no. 3, pp. 146-152, 2001.

[13] H. Al-Nimry and A. Soman, "On The Slenderness and FRP Confinement Of Eccentrically-Loaded Circular RC Columns," *Engineering Structures,* vol. 164, pp. 92-108, 2018.

[14] ACI 440.2R, "Guide for the Design and Construction of Externally Bonded FRP Systems for Strengthening Concrete Structures," American Concrete Institute, Farmington Hills, MI, 2017.

[15] T. C. Triantafillou and N. Plevris, "Strengthening of RC beams with Epoxy-Bonded Fibre-Composite Materials," *Materials and Structures,* vol. 25, pp. 201-211, 1992.

[16] A. Sharif, G. J. Al-Sulaimani, I. A. Basunbul, M. H. Baluch and B. N. Ghaleb, "Strengthening of Initially Loaded Reinforced Concrete Beams Using FRP Plates," *ACI Structural Journal,* vol. 91, no. 2, pp. 160-168, 1994.

[17] M. Shahawy, M. Arockiasamy, T. Beitelman, and R. Sowrirajan, "Reinforced Concrete Rectangular Beams Strengthened with CFRP Laminates," *Composites Part B: Engineering,* vol. 27, no. 3-4, pp. 225-233, 1996.

[18] O. Buyukozturk and B. Hearing, "Failure Behavior of Precracked Concrete Beams Retrofitted with FRP," *Journal of composites for construction,* pp. 138-144, 1998.

[19] A. M. Malek, H. Saadatmanesh and M. R. Ehsani, "Prediction of Failure Load Of R/C Beams Strengthened with FRP Plate Due to Stress Concentration at The Plate End," *ACI Structural Journal,* pp. 142-152, 1998.

[20] H. Rahimi and A. Hutchinson, "Concrete Beams Strengthened with Externally Bonded FRP Plates," *Journal of composites for construction,* pp. 44-56, 2001.

[21] A. F. Ashour, S. A. El-Refaie and S. W. Garrity, "Flexural Strengthening of RC Continuous Beams using CFRP Laminates," *Cement and concrete composites,* vol. 26, no. 7, pp. 765-775, 2004.

[22] A. S. Mosallam and K. M. Mosalam, "Strengthening of Two-Way Concrete Slabs with FRP Composite Laminates," *Construction and Building Materials,* vol. 17, no. 1, pp. 43-54, 2003.

[23] Y. J. Kim, J. M. Longworth, and G. R. Wight, "Flexure of Two-Way Slabs Strengthened with Prestressed or Nonprestressed CFRP Sheets," *Journal of Composites for Construction,* vol. 12, no. 4, pp. 366-374, 2008.

[24] T. Alkhrdaji, A. Nanni, G. Chen, and M. Barker, "Upgrading the Transportation Infrastructure: Solid RC Decks Strengthened with FRP," *Concrete International: Design and Construction,* vol. 21, no. 10, pp. 37-41, 1999.

[25] H. Tarek and S. Rizkalla, "Flexural Strengthening of Prestressed Bridge Slabs with FRP systems," *PCI Journal,* vol. 47, no. 1, pp. 76-93, 2002.

[26] R. Atadero, L. Lee and V. M. Karbhari, "Consideration of material variability in Reliability Analysis of FRP Strengthened Bridge Decks," *Composite Structures,* vol. 70, no. 4, pp. 430-443, 2005.

[27] CAN/CSA S806-12, "Design and construction of building structures with Fibre-Reinforced Polymers," Canadian Standards Association, 2012.

[28] K. Gadjosova and J. Bilcik, "Full-scale testing of CFRP-strengthened slender reinforced concrete columns," *Journal of composites for construction,* vol. 17, pp. 239-248, 2013.

[29] P. Sadeghian and . A. Fam, "Strengthening Slender Reinforced Concrete Columns Using High-Modulus Bonded Longitudinal Reinforcement for Buckling Control," *Journal of Structural Engineering,* vol. 141, p. 04014127, 2015.

[30] K. Khorramian and P. Sadeghian, "Rehabilitation of Bridge Columns Using Hybrid Strengthening Method of Longitudinal CFRP and Transverse GFRP Wraps," in *10th International Conference on Short and Medium Span Bridges*, Quebec City, Quebec, Canada, 2018.

[31] K. Khorramian and P. Sadeghian, "Strengthening Concrete Columns Using Near Surface Mounted (NSM) Carbon Fiber Reinforced Polymer (CFRP) Laminates," in *Sixth Asia-Pacific Conference on FRP in Structures*, Singapore, Singapore, 2017.

[32] K. Khorramian and P. Sadeghian, "Strengthening Short Concrete Columns Using Longitudinally Bonded CFRP Laminates," *ACI Special Publication,* vol. 327, pp. 24-1, 2018.

[33] K. Khorramian and P. Sadeghian, "Strengthening of Slender Circular Concrete Columns with Longitudinal CFRP Laminates and Transverse GFRP wraps," in *CSCE Annual Conference*, Fredericton, NB, Canada, 2018.

[34] K. Khorramian and P. Sadeghian, "Performance of high-Modulus Near-Surface-Mounted FRP Laminates for Strengthening of Concrete Columns," *Composites Part B,* vol. 164, pp. 90-102, 2019.

[35] M. H. Abdallah, H. M. Mohamed, and R. Masmoudi, "Experimental Assessment and Theoretical Evaluation of Axial Behavior of Short and Slender CFFT Columns Reinforced with Steel and CFRP Bars," *Construction and Building Materials,* vol. 181, p. 535–550, 2018.

[36] M. Chellapandian, S. Suriya Prakash and A. Raj, "Analytical and Finite Element Studies on Hybrid FRP Strengthened RC Column Elements under Axial and Eccentric Compression," *Composite Structures,* vol. 184, pp. 234-248, 2018.

[37] Y. A. Al-Salloum, G. S. Al-Amri, N. A. Siddiqui, T. H. Almusallam and H. Abbas, "Effectiveness of CFRP Strengthening in Improving Cyclic Compression Response of Slender RC Columns," *Journal of Composites for Construction,* vol. 22, no. 3, p. 04018009, 2018.

[38] H. Tobbi, A. S. Farghaly and B. Benmokrane, "Concrete Columns Reinforced Longitudinally and Transversally with Glass Fiber-Reinforced Polymer Bars," *ACI Structural Journal,* vol. 109, no. 4, pp. 551-558, 2012.

[39] H. M. Mohamed, M. Z. Afifi and B. Benmokrane, "Performance Evaluation of Concrete Columns Reinforced Longitudinally with FRP Bars and Confined with FRP Hoops and Spirals under Axial Load," *Journal of Bridge Engineering,* vol. 19, no. 7, p. 04014020, 2014.

[40] K. Khorramian and P. Sadeghian, "Experimental and Analytical Behavior of Short Concrete Columns Reinforced with GFRP Bars under Eccentric Loading," *Engineering Structures,* vol. 151, p. 761–773, 2017.

[41] K. Khorramian and P. Sadeghian, "New Testing Method of GFRP Bars in Compression," in *CSCE Annual Conference*, Fredericton, NB, Canada, 2018.

[42] K. Khorramian and P. Sadeghian, "Material Characterization of GFRP Bars in Compression using a New Test Method," *Journal of Testing and Evaluation (ASTM),* pp. in-Press, 2019.

[43] K. Khorramian and P. Sadeghian, "Short Concrete Columns Reinforced with GFRP Rebars Under Eccentric Loading," in *CSCE annual conference*, Vancouver, Canada, 2017.

[44] B. Fillmore and P. Sadeghian, "Contribution of Longitudinal Glass Fiber-Reinforced Polymer Bars in Concrete Cylinders under Axial Compression," *Canadian Journal of Civil Engineering,* vol. 45, pp. 458-468, 2018.

[45] M. Guérin, H. M. Mohamed, B. Benmokrane, A. Nanni and C. K. Shield, "Eccentric Behavior of Full-Scale Reinforced Concrete Columns with Glass Fiber-Reinforced Polymer Bars and Ties," *ACI Structural Journal,* vol. 115, no. 2, pp. 489-499, 2018.

[46] M. Elchalakani, A. Karrech, M. Dong, M. M. Ali and B. Yang, "Experiments and Finite Element Analysis of GFRP Reinforced Geopolymer Concrete Rectangular Columns Subjected to Concentric and Eccentric Axial Loading," *Structures,* vol. 14, pp. 273-289, 2018.

[47] W. Xue, F. Peng, and Z. Fang, "Behavior and Design of Slender Rectangular Concrete Columns Longitudinally Reinforced with Fiber-Reinforced Polymer Bars," *ACI Structural Journal,* vol. 115, no. 2, pp. 311-322, 2018.

[48] O. Chaallal and M. Shahawy, "Performance of Fiber-Reinforced Polymer-Wrapped Reinforced Concrete Column under Combined Axial-Flexural Loading," *ACI Structural Journal,* vol. 97, no. 4, pp. 659-668, 2000.

[49] A. Shaat and A. Z. Fam, "Slender Steel Columns Strengthened Using High-Modulus CFRP Plates for Buckling Control," *Journal of Composites for Construction,* vol. 13, no. 1, pp. 2-12, 2009.

[50] N. A. Siddiqui, S. H. Alsayed, Y. A. Al-Salloum, R. A. Iqbal and H. Abbas, "Experimental Investigation of Slender Circular RC Columns Strengthened with FRP Composites," *Construction and Building Materials,* vol. 69, p. 323–334, 2014.

[51] ASTM D3039/D3039M-14, "Standard Test Method for Tensile Properties of Polymer Matrix Composite Materials," American Society for Testing and Materials, West Conshohocken, PA, 2014.

[52] ASTM D6641/D6641M-16, "Standard Test Method for Compressive Properties of Polymer Matrix Composite Materials Using a Combined Loading Compression (CLC) Test Fixture," American Society for Testing and Materials, West Conshohocken, PA, 2016.

[53] S. Popovics, "A Numerical Approach to the Complete Stress-Strain Curve of Concrete," *Cement and concrete research,* vol. 3, no. 5, pp. 583-599, 1973.

[54] ACI 318-19, "Building Code Requirements for Structural Concrete," American Concrete Institute, Farmington Hills, MI, 2019.

[55] K. Khorramian and P. Sadeghian, "Behavior of Slender GFRP Reinforced Concrete Columns," in *ASCE-SEI Structures Congress, American Society of Civil Engineers*, St. Louis, Missouri, USA, 2019.

[56] K. Khorramian and P. Sadeghian, "Experimental Investigation of Short and Slender Rectangular Concrete Columns Reinforced with GFRP Bars under Eccentric Axial Loads," *Journal of Composites for Construction,* p. under review, 2020.

[57] G. Lin and J. G. Teng, "Stress-Strain Model for FRP-Confined Concrete in Eccentrically Loaded Circular Columns," *Journal of Composites for Construction,* vol. 23, no. 3, p. 04019017, 2019.

[58] M. R. Spoelstra and G. Monti, "FRP-Confined Concrete Model," *Journal of Composites for Construction,* vol. 3, no. 3, pp. 143-150, 1999.

[59] L. Lam and J. G. Teng, "Design-Oriented Stress-Strain Model for FRP-Confined Concrete,"

Construction and building materials, vol. 2003, no. 6-7, pp. 471-489, 2003.

Table 1–Test matrix for phase I.

No.	Specimen ID	Longitudinal Reinforcement	Transverse Reinforcement	Reinforcement Code
1	P-w0-1	-	-	
2	P-w0-2	-	-	Plain Concrete
3	P-w0-3	-	-	
4	L-w0-1	16 CFRP strips	-	
5	L-w0-2	16 CFRP strips	-	Longitudinal reinforcement only
6	L-w0-3	16 CFRP strips	-	
7	T-w2-1	-	2 layer GFRP wrap	
8	T-w2-2	-	2 layer GFRP wrap	Transverse with 2 layer wrapping
9	T-w2-3	-	2 layer GFRP wrap	
10	H-w2-1	16 CFRP strips	2 layer GFRP wrap	
11	H-w2-2	16 CFRP strips	2 layer GFRP wrap	Hybrid with 2 layer wrapping
12	H-w2-3	16 CFRP strips	2 layer GFRP wrap	
13	T-w4-1	-	4 layer GFRP wrap	
14	T-w4-2	-	4 layer GFRP wrap	Transverse with 4 layer wrapping
15	T-w4-3	-	4 layer GFRP wrap	
16	H-w4-1	16 CFRP strips	4 layer GFRP wrap	
17	H-w4-1	16 CFRP strips	4 layer GFRP wrap	Hybrid with 4 layer wrapping
18	H-w4-3	16 CFRP strips	4 layer GFRP wrap	

Table 2–Material properties.

No.	Material Type	f_t (MPa)	E (GPa)	ε_t (mm/mm)	F_b (MPa)
1	CFRP laminate in tension	3267	177.8	0.0179	-
2	CFRP laminate in compression	1086	152.9	0.0071	-
3	GFRP wrap	391	25.7	0.0152	-
4	Bonding adhesive	25	4.4	0.0100	21.3
5	Epoxy resin	50	2.8	0.0450	-

Note: *= properties in compression are reported; f_t = ultimate tensile strength; E = modulus of elasticity; ε_t = ultimate tensile strain; F_b = bond strength.

Table 3–Summary of test results for phase I.

Group	Specimen ID	Strength (kN)	SG on CFRP	SG on GFRP		LP	
			$\varepsilon_{Axial\text{-}SG\text{-}C}$	$\varepsilon_{Axial\text{-}SG\text{-}G}$	$\varepsilon_{Lateral\text{-}SG}$	$\varepsilon_{Axial\text{-}LP}$	$\varepsilon_{Lateral\text{-}LP}$
Plain	P1	965.0	-	-	-	0.00300	0.00268
	P2	1046.9	-	-	-	0.00281	0.00275
	P3	1001.1	-	-	-	0.00295	0.00116
Longitudinal	L1	1099.8	0.00240	-	-	0.00094	0.00231
	L2	1183.0	0.00256	-	-	0.00158	0.00207
	L3	1199.7	0.00244	-	-	0.00191	0.00207
Transverse 2 layer wrap	T1-2w	1188.3	-	0.00374	0.01422	0.00788	0.01530
	T2-2w	1226.7	-	0.00678	0.01329	0.00895	0.01365
	T3-2w	1324.3	-	0.00932	0.01480	0.01193	0.01623
Hybrid 2 layer wrap	H1-2w	1280.3	0.00140	-	-	0.00292	0.00311
	H2-2w	1215.8	-	-	-	0.00297	0.01271
	H3-2w	1328.1	-	0.00320	0.00204	0.00302	0.00208
Transverse 4 layer wrap	T1-4w	1733.2	-	0.00985	0.01864	0.01285	0.01657
	T2-4w	1731.2	-	0.01405	0.01607	0.01309	0.01874
	T3-4w	1819.8	-	0.01751	0.01678	0.01477	0.02049
Hybrid 4 layer wrap	H1-4w	1712.5	-	-	0.01061	0.00865	0.00459
	H2-4w	1605.4	-	0.00477	0.01186	0.01011	0.00816
	H3-4w	1783.4	-	0.00635	0.01408	0.00629	0.01202

Note: $\varepsilon_{Axial\text{-}SG\text{-}C}$ = average axial strain gauge recording on CFRP strips; $\varepsilon_{Axial\text{-}SG\text{-}G}$ = average axial strain gauge recording on GFRP wrapping; $\varepsilon_{Lateral\text{-}SG}$ = average lateral strain gauge recording on GFRP wrapping; $\varepsilon_{Axial\text{-}LP}$ = average axial strain calculated from the recording of longitudinal LPs; $\varepsilon_{Lateral\text{-}LP}$ = equivalent lateral strain calculated from the recording of lateral LPs.

Table 4–Average test results at peak load for phase I.

Group	P_u (kN)	Gain in Capacity (%)	ε_{long} (mm/mm)	$\Delta\varepsilon_{long}$ (mm/mm)	ε_{lat} (mm/mm)	$\Delta\varepsilon_{lat}$ (mm/mm)
Plain	1004.3	-	0.00292	-	0.00219	-
Longitudinal	1160.8	15.6	0.00197	-0.00095	0.00215	-0.00004
Transverse 2 layer wrap	1246.5	24.1	0.00810	0.00518	0.01458	0.01239
Hybrid 2 layer wrap	1274.7	26.9	0.00270	-0.00022	0.00499	0.00279
Transverse 4 layer wrap	1761.4	75.4	0.01369	0.01077	0.01788	0.01569
Hybrid 4 layer wrap	1700.4	69.3	0.00723	0.00431	0.01022	0.00803

Note: P_u = average of peak loads; ε_{long} = average longitudinal strain; ε_{lat} = average lateral strain; $\Delta\varepsilon_{long}$ = the additional longitudinal strain with respect to the plain group; $\Delta\varepsilon_{lat}$ = the additional lateral strain with respect to plain group.

Table 5–Confinement Effect for phase I.

No.	Specimen ID	t_f (mm)	f'_{cc} (MPa)	f_{cc}/f'_{co}	$\varepsilon_{h,rup}$ (%)	$\varepsilon_{h,rup}/\varepsilon_{frp}$	f_l (MPa)	$f_{l,0.55}$ (MPa)	$f_{l,hr}$ (MPa)	f_l/f'_{co}	$f_{l,0.55}/f'_{co}$	$f_{l,hr}/f'_{co}$
1	T-w2-1	1.08	67.2	1.18	1.80	1.19	5.63	3.09	6.67	0.10	0.05	0.12
2	T-w2-2	1.08	69.4	1.22	1.40	0.92	5.63	3.09	5.17	0.10	0.05	0.09
3	T-w2-3	1.08	74.9	1.32	1.66	1.09	5.63	3.09	6.14	0.10	0.05	0.11
4	H-w2-1	1.08	63.6	1.12	0.38	0.25	5.63	3.09	1.40	0.10	0.05	0.02
5	H-w2-2	1.08	56.6	1.00	1.15	0.76	5.63	3.09	4.26	0.10	0.05	0.08
6	H-w2-3	1.08	62.4	1.10	0.91	0.60	5.63	3.09	3.37	0.10	0.05	0.06
7	T-w4-1	2.16	98.1	1.73	1.85	1.22	11.25	6.19	13.70	0.20	0.11	0.24
8	T-w4-2	2.16	98.0	1.72	1.74	1.15	11.25	6.19	12.89	0.20	0.11	0.23
9	T-w4-3	2.16	103.0	1.81	1.87	1.23	11.25	6.19	13.86	0.20	0.11	0.24
10	H-w4-1	2.16	61.4	1.08	0.76	0.50	11.25	6.19	5.63	0.20	0.11	0.10
11	H-w4-2	2.16	60.3	1.06	1.00	0.66	11.25	6.19	7.41	0.20	0.11	0.13
12	H-w4-3	2.16	75.0	1.32	1.31	0.86	11.25	6.19	9.66	0.20	0.11	0.17

Note: $\varepsilon_{h,rup}$ = hoop rupture strain of GFRP wrapping read from column test; ε_{frp} = the ultimate tensile strain of GFRP wrap from tensile coupon tests; $f_{l,hr}$ = confining pressure calculated using $\varepsilon_{h,rup}$; $f_{l,0.55}$ = confining pressure calculated using 0.55 ε_{frp}; f_l = confining pressure calculated using ε_{frp}.

Table 6–Test matrix for phase II.

No.	Specimen ID	D (mm)	L (mm)	λ	e/D	Steel Reinforcement	Transverse Reinforcement	Longitudinal Reinforcement
1	Control	260	3048	47	0.15	6-15M	-	-
2	Wrapped	260	3048	47	0.15	6-15M	6 layer GFRP wrap	-
3	Hybrid	260	3048	47	0.15	6-15M	6 layer GFRP wrap	16 CFRP strips

Note: D = diameter of column; L = length of column; λ = slenderness ratio; e = load eccentricity.

Table 7–Summary of test results for phase II.

No.	Specimen ID	P_u (kN)	M_u (kN-m)	Δ_u (mm)	$\varepsilon_{Axial\text{-}Steel}$		$\varepsilon_{Hoop\text{-}FRP}$	
					Comp.	Ten.	Comp.	Ten.
1	Control	1127.5	64.12	16.87	0.0022	-0.0003	-	-
2	Wrapped	1334.8	84.30	23.15	0.0023	-0.0008	0.0024	-0.0008
3	Hybrid	1920.8	151.51	38.88	0.0020	-0.0016	0.0050	-0.0027

Note: P_u = the peak load; M_u = the bending moment corresponding to the peak load; Δ_u = the lateral displacement corresponding to the peak load; $\varepsilon_{Axial\text{-}Steel}$ = the axial strain of steel at the peak load; $\varepsilon_{Hoop\text{-}FRP}$ = the hoop direction strain of GFRP wrapping at the peak load;
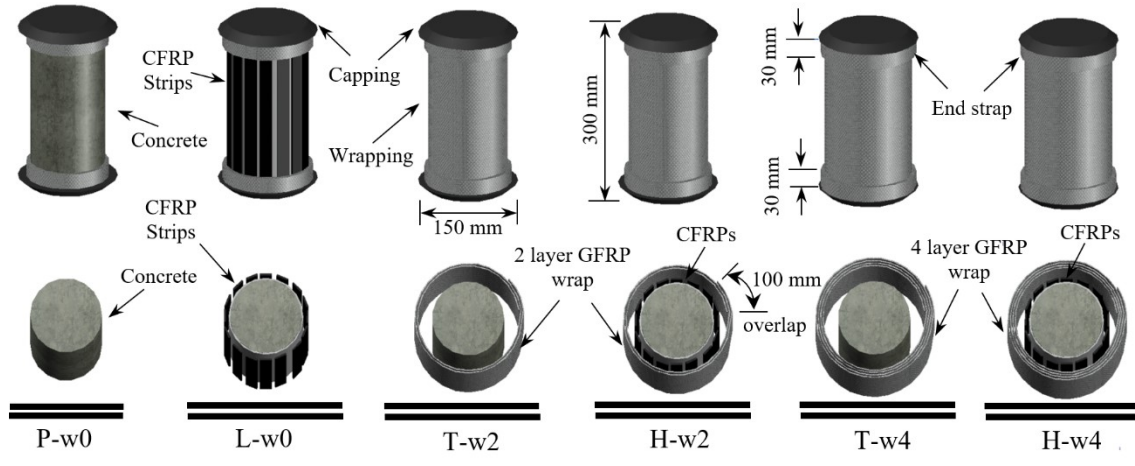
Fig. 1–Groups of specimens for phase I.
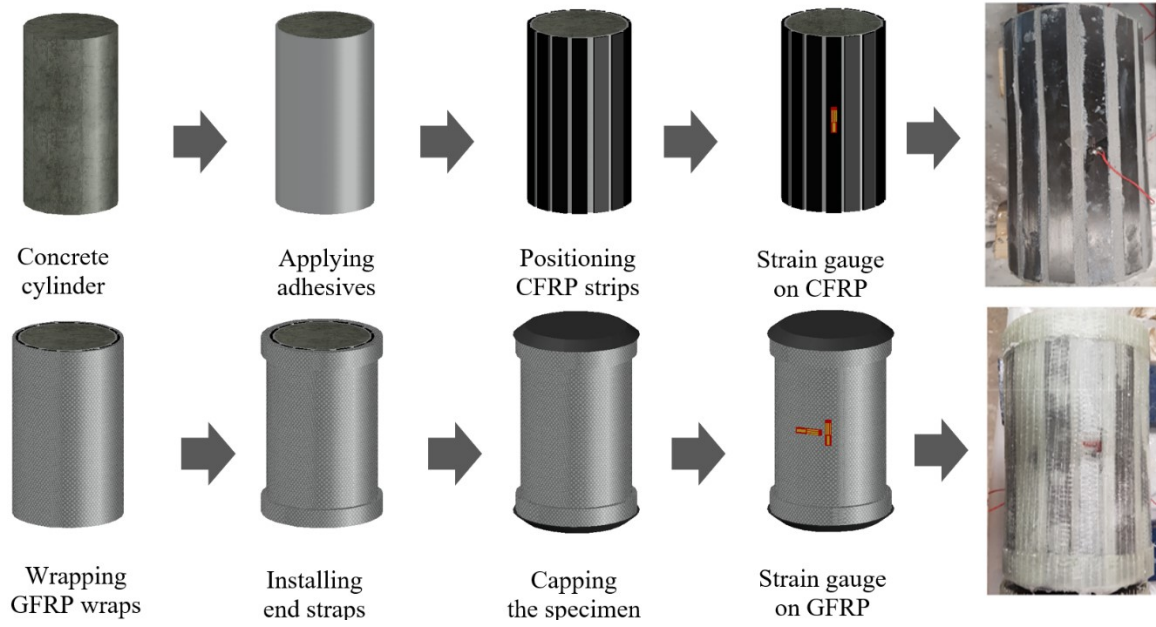
Fig. 2–Fabrication process for phase I.
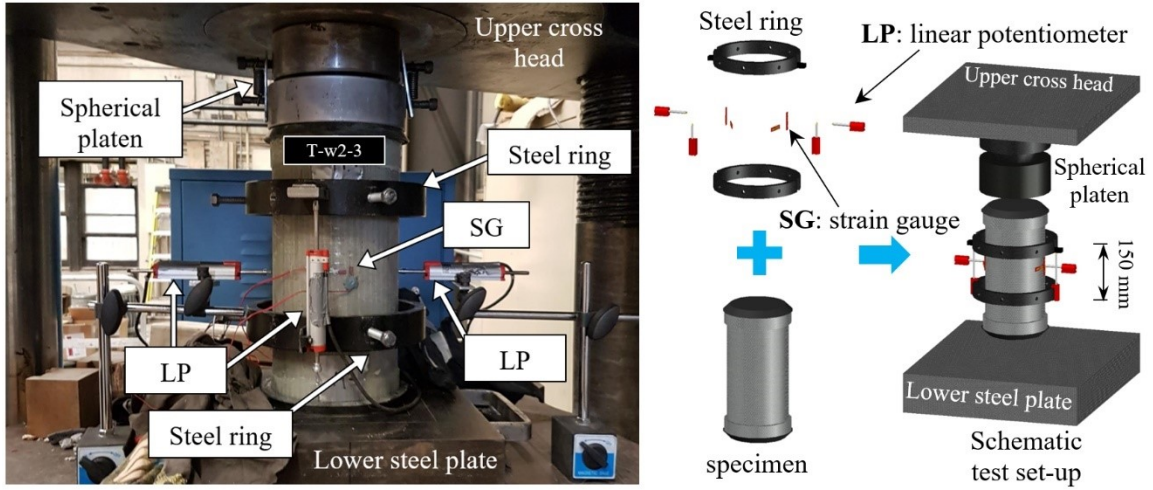
Fig. 3–Test set-up and instrumentation for phase I.
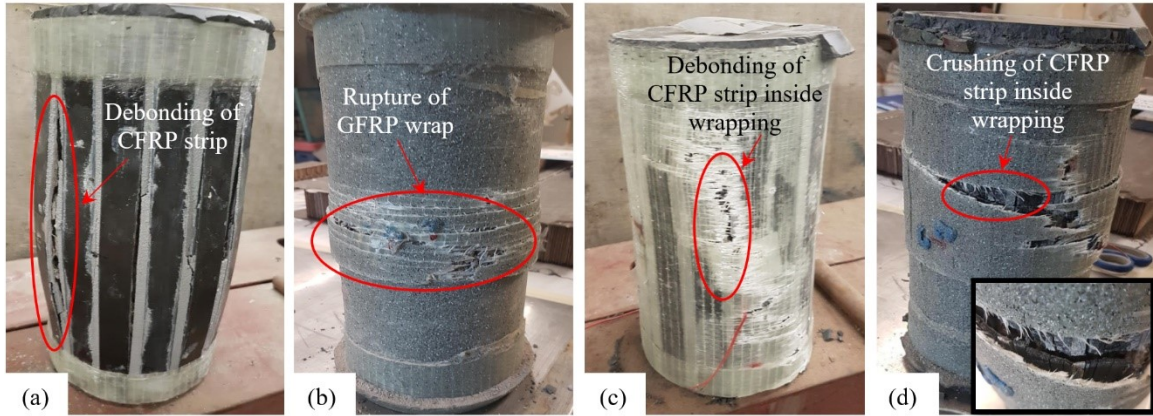
Fig. 4–Typical failure modes of phase I: (a) L-w0-1; (b) T-w4-1; (c) H-w2-1; and (d) H-w4-1.
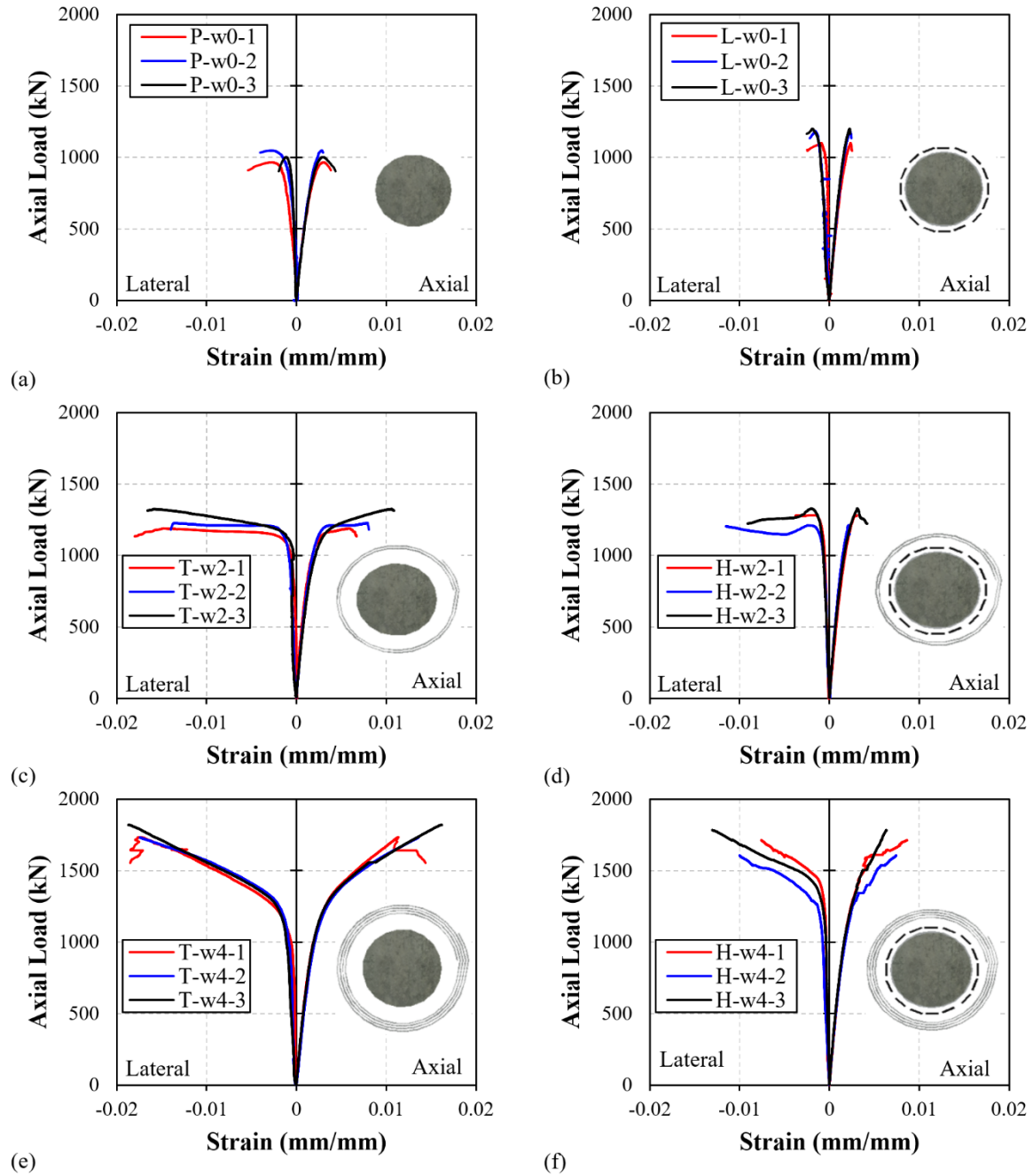
Fig. 5–Load-strain curves: (a) P-w0; (b) L-w0; (c) T-w2; (d) H-w2; (e) T-w4; and (f) H-w4.
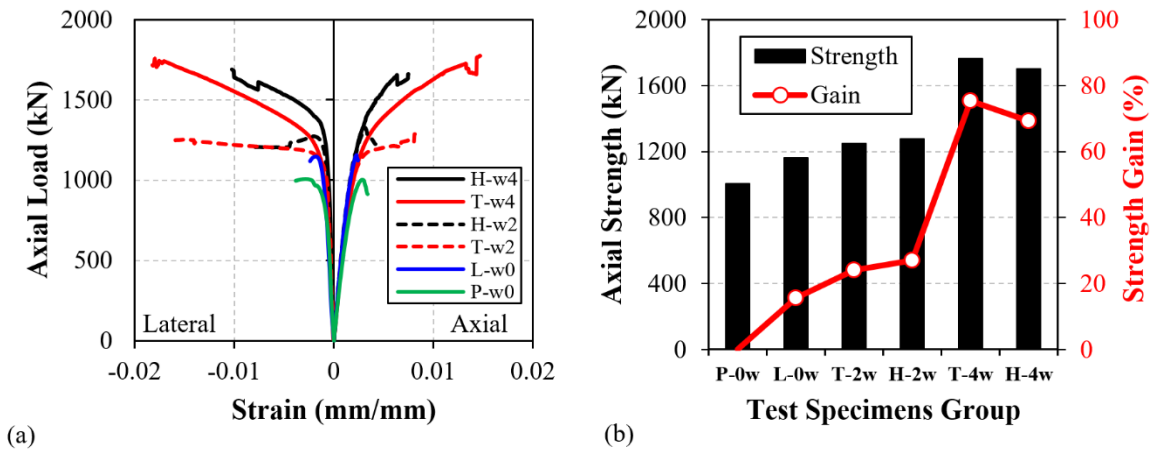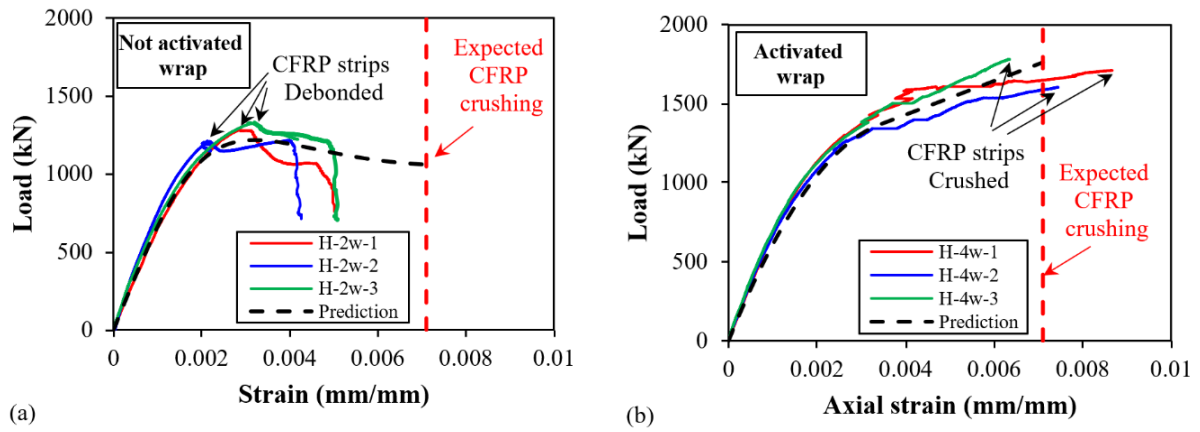
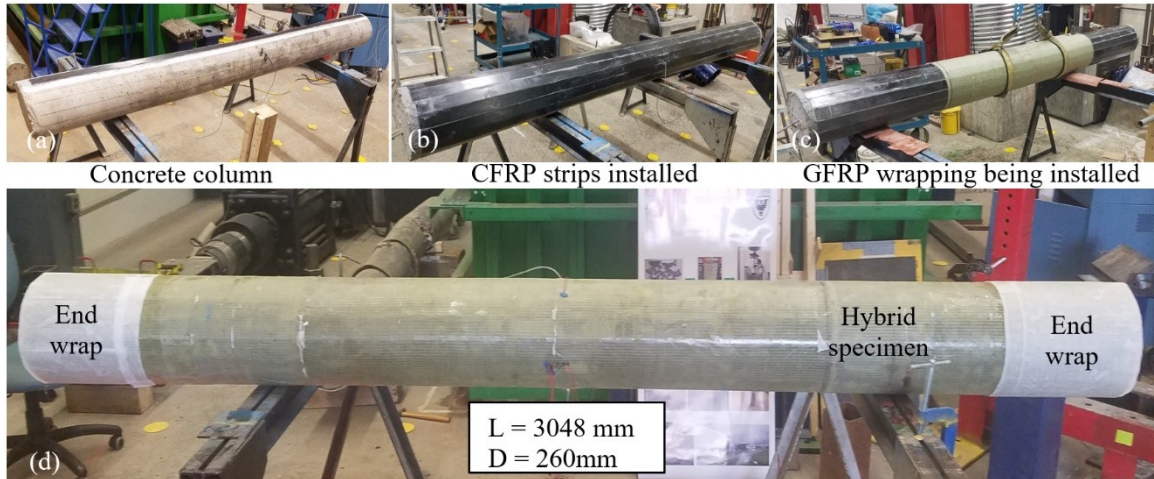**Fig. 6–Summary of test results for phase I: (a) average load-strain curves; and (b) average compressive strength.**
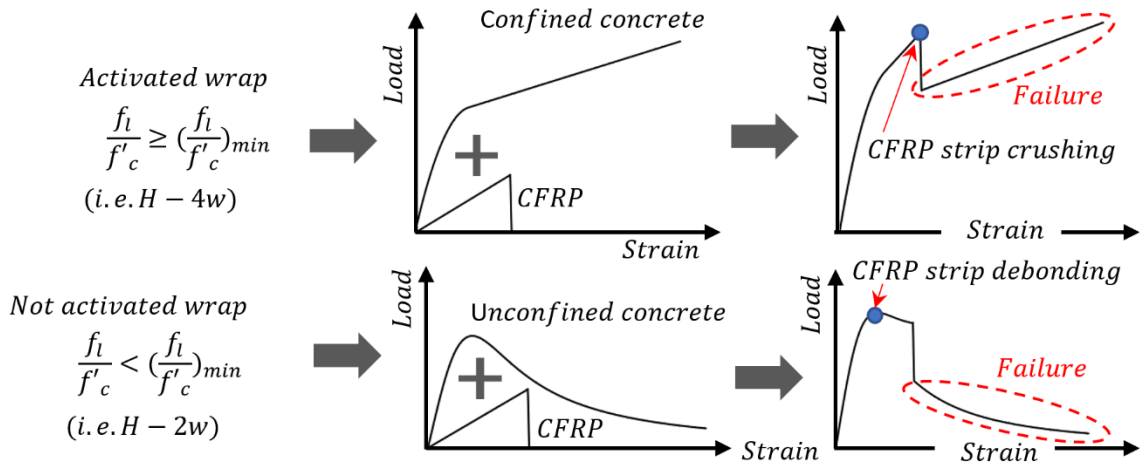
Fig. 7– Mechanics of the hybrid system for phase I.

Fig. 8–Verification of the predictions based on the hybrid system mechanism for phase I: (a) Specimen H-2w without activated wrap; and (b) Specimen H-4w with activated wrap.

Fig. 9–Specimen preparation for phase II: (a) slender concrete column; (b) specimen with CFRP strips installed; (c) specimen with GFRP wrapping is being installed; and (d) hybrid specimen with end wrapping.
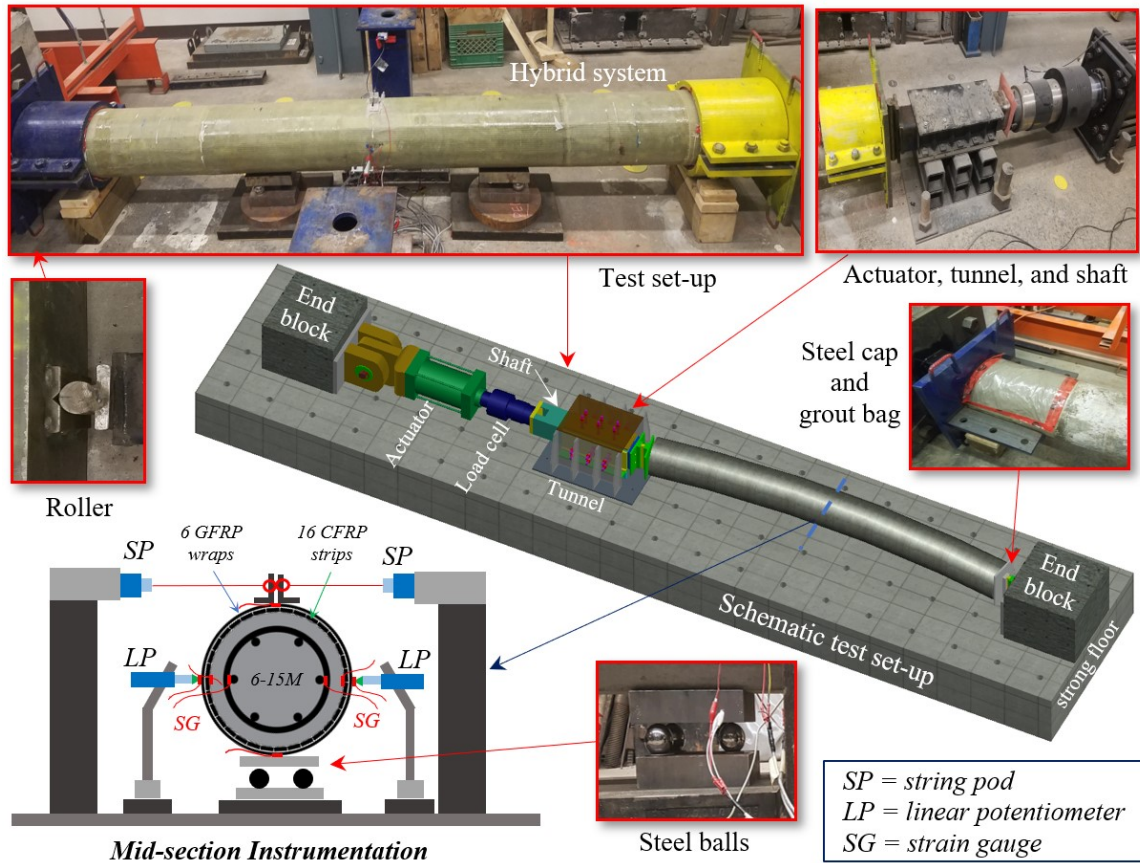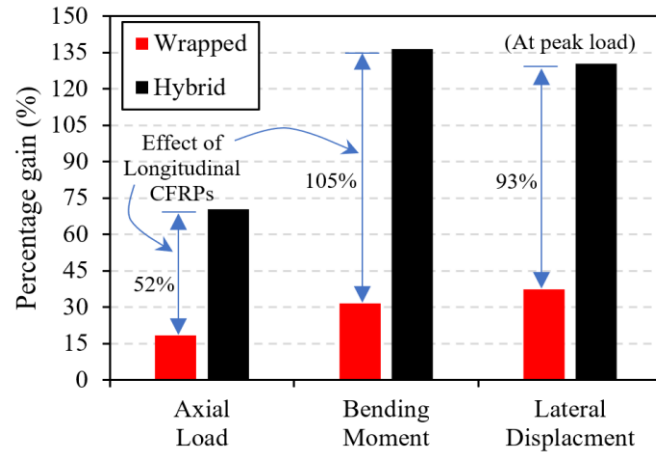
Fig. 10–Test set-up and instrumentation for phase II.
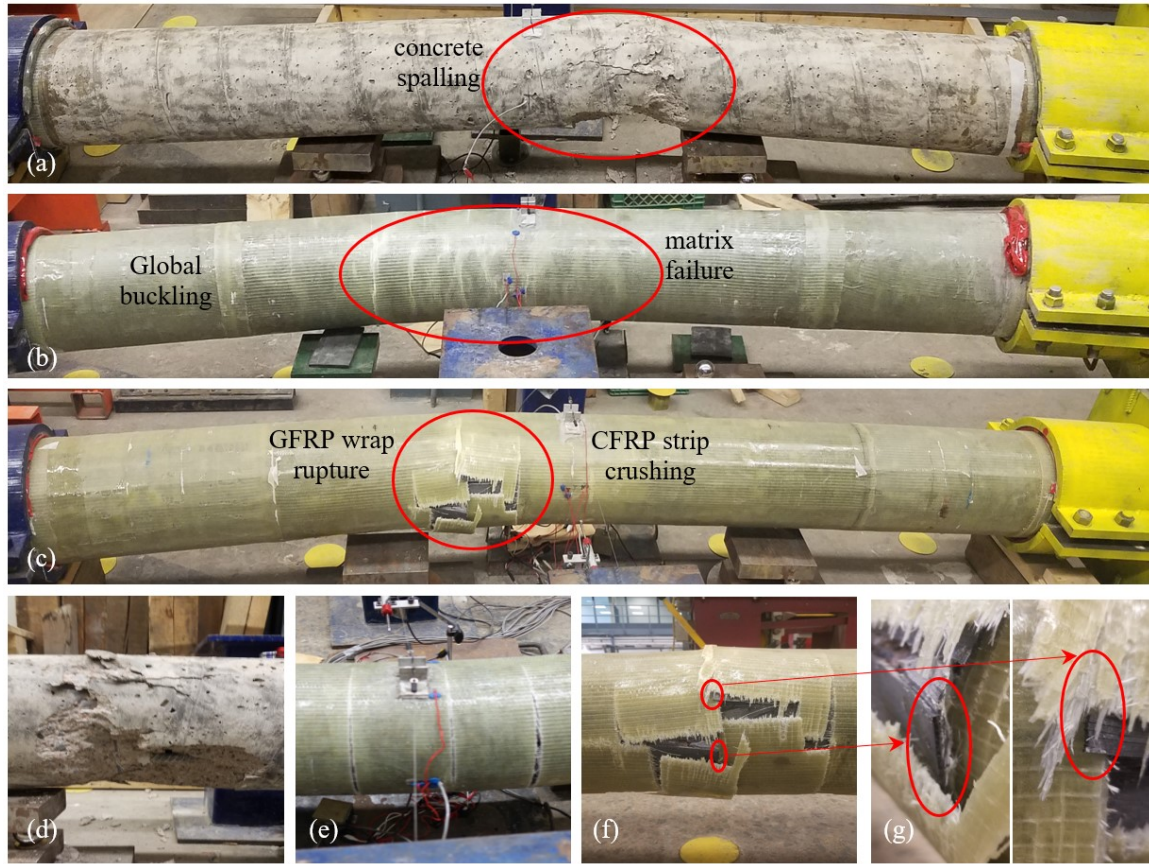
Fig. 11–Failure modes for phase II: (a) failed control specimen; (b) failed wrapped specimen; (c) failed hybrid specimen; (d) concrete spalling; (e) matrix rupture; (f) rupture of GFRP wrap; and (g) crushing of CFRP strip.
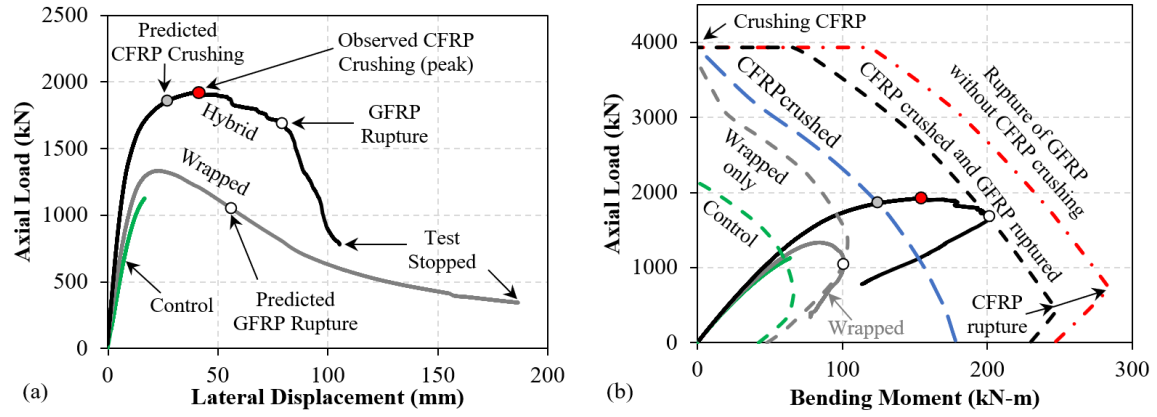
Fig. 12– Test results for phase II: (a) axial load-lateral displacement; and (b) axial load-bending moment.

Fig. 13– Percentage gain of capacity with respect to the control specimen for phase II.